DESIGN, DEVELOPMENT, AND MANUFACTURING OF REFRACTORY METALS & MATERIALS

Paralinear Oxidation of Cr-Si-C-Coated C/SiC at 1300°C in Wet and Dry Air Environments

SHOUJUN WU,[1,2,5] SHAOJUN MA,[2] YINGXIN CHEN,[2]
BAOWEI CAO,[3] and GUOYUN ZHANG[4]

1.—Key Laboratory of Agricultural Soil and Water Engineering in Arid and Semiarid Areas, Ministry of Education, Northwest A&F University, Yangling 712100, China. 2.—College of Water Resources and Architectural Engineering, Northwest A&F University, Yangling 712100, Shaanxi, People's Republic of China. 3.—School of Chemistry and Chemical Engineering, Yulin University, Yulin 719000, Shaanxi, People's Republic of China. 4.—State Key Laboratory of Crop Stress Biology for Arid Areas, Northwest A&F University, Yangling 712100, Shaanxi, People's Republic of China. 5.—e-mail: shoujun_wu@163.com

The oxidation kinetics of a Cr_3Si-Cr_7C_3/SiC/SiC-coated C/SiC were comparatively investigated in dry and wet air at 1300°C under 1 atm. After oxidation for 10 h, Cr_2O_3 and SiO_2 were produced in both oxidations. However, a larger amount of SiO_2 formed during the wet air oxidation. After the dry air oxidation, the surface of Cr_3Si-Cr_7C_3/SiC/SiC coating became relatively loose with many pores. After the wet air oxidation, the surface of Cr_3Si-Cr_7C_3/SiC/SiC coating became undulating and loose with notable damage at the position of bulges. The Cr_3Si-Cr_7C_3/SiC/SiC-coated C/SiC showed paralinear weight gains in both oxidation environments. Although the initial weight gains within the first 1 h in the wet air oxidation condition were higher, the gradual weight gains thereafter were lower. The parabolic rate constant for oxide formation and the linear rate constant for oxide volatilization in the wet air oxidation condition were higher than those in the dry air oxidation condition.

INTRODUCTION

Continuous carbon fiber-reinforced silicon carbide (C/SiC) composites are one of the most promising thermostructural materials for high-temperature heat exchangers, hot gas filters, turbine engines, spacecraft reentry thermal protection systems, and ultra-lightweight mirrors, etc.[1–5] Most of these applications operate under high-temperature oxidizing environments, even containing water vapor, such as combustor liners, turbine vanes and thrusters for propulsion.

The oxidation of SiC in air is passive up to 1700°C and the formed SiO_2 film has a low oxygen diffusion coefficient. Chemical vapor-deposited (CVD) SiC has been predominantly used as the coating material to protect thermal structural composites from oxidation.[6–10] However, below the deposition temperature (usually 1000°C), oxidizing agents can diffuse inward through microcracks mainly produced by mismatch in the coefficient of thermal expansion (CTE) between the composite and the coating,

leading to oxidation of the carbon phases in the composite.[7,8] Earlier work has demonstrated that, compared to a SiC/SiC/SiC coating, a Cr_3Si-Cr_7C_3/SiC/SiC coating showed enhanced oxidation protection because of the formation of a protective Cr_2O_3 layer below 1000°C and a SiO_2 layer at high temperatures.[11] It has been confirmed that oxidation of SiC and Cr_2O_3 formers, such as chromium, chromium carbides and chromium silicides in dry air are different from those in wet air.[12–16] Research has confirmed that water vapor strongly enhances the oxidation rate of SiC.[12, 13] At temperatures from 1100°C to 1300°C, oxide growth of iron-chromium-aluminum alloys (FeCrAl) in dry air was faster than that in wet air.[14] It has been well acknowledged that water vapor can not only accelerate formation of Cr_2O_3 but also enhance its vaporization.[17–20] It has been revealed that Cr_2O_3 evaporates linearly with time in N_2-O_2-H_2O atmospheres, and that the evaporation rate increases with temperature.[19] Therefore, above 1000°C, the oxidation behavior of the Cr_3Si-Cr_7C_3/SiC/SiC coating in wet air might

differ from that in dry air. Unfortunately, reports on the comparisons of the oxidation of the Cr_3Si-Cr_7C_3/SiC/SiC coating above 1000°C in dry and wet air, especially on the oxidation kinetics and oxidation rate, are lacking.

The present work deals with the high-temperature oxidation behavior of a Cr_3Si-Cr_7C_3/SiC/SiC coating investigated in dry air and in 18 vol.% O_2 + 72 vol.% N_2 +10 vol.% H_2O under 1 atm with a flow rate of 3.0 cm s^{-1} at 1300°C. Much of the analysis and discussion are mainly focused on the differences in the oxidation kinetics, micromorphologies of the coating, the parabolic rate constant for oxide formation, and the linear rate constant for oxide volatilization.

EXPERIMENTAL PROCEDURE

Preparation of Samples

A two-dimensional C/SiC composite prepared by low-pressure chemical vapor infiltration was used as the substrate. The preform was laid up with polyacrylonitrile (PAN)-based carbon fiber clothes (T300^{TM}). After deposition of a pyrolytic carbon (PyC) interface layer using butane, the preform was deposited with a SiC matrix using methyltrichlorosilane (MTS). The deposition conditions for the PyC interface layer were as follows: temperature 960°C, pressure 5 kPa, time 20 h, Ar flow 200 mL min^{-1}, and C_4H_{10} flow 15 mL min^{-1}. The deposition conditions for the SiC matrix were as follows: temperature 1000°C, pressure 5 kPa, time 120 h, H_2 flow 350 mL min^{-1}, Ar flow 350 mL min^{-1}, and the molar ratio of H_2 to MTS was 10:1. The as-received composite was cut and machined to obtain substrates with a size of 3.0 mm × 4.0 mm × 30 mm.

The obtained composite substrates were initially coated with two layers of SiC by CVD, then an additional Cr_3Si-Cr_7C_3 coating was prepared using a powder immersion reaction-assisted coating (PIRAC) method. The conditions for the CVD SiC deposition were the same as that for the SiC matrix, except that the deposition time was 30 h per cycle. In the PIRAC processing, samples with two layers of SiC coatings were inside sealed into a Cr-rich stainless steel container packed with Cr powders. They were then sealed into an additional Cr-rich stainless steel container with small amounts of titanium and chromium powder, acting as getters for N_2 and O_2, respectively. They were finally annealed at 1000°C for 2 h to form a Cr_3Si-Cr_7C_3 coating via the reaction of Cr and SiC.[11] The prepared coating is referred to as the Cr_3Si-Cr_7C_3/SiC/SiC coating. A schematic of the sample fabrication processes is shown in Fig. 1.

Oxidation Tests

Oxidation tests were conducted in dry air (composed of 22 vol.% O_2 and 78% vol.% N_2) and wet air at 1300°C under 1 atm. The wet air oxidation tests were carried out in 18 vol.% O_2 + 72.% vol.% N_2 +10 vol.% H_2O atmosphere. Deionized water was used to generate water vapor. In each test, three specimens were placed into an alumina tube with a purity of 99.99% at the desired temperature, and then the mixed gas flow was introduced into the alumina tube. The velocity of the mixed gas was 3.0 cm s^{-1} to minimize the volatility of the SiO_2 scale formed on the SiC coating. The masses of the specimens before and after oxidation were measured using an electronic analytical balance (resolution: 0.01 mg).

Characterization of Phase Composition and Microstructure

Phase composition and microstructure of the samples were characterized using x-ray diffraction (XRD; BRUKER, D8 ADVANCE A25 X) and scanning electron microscopy (SEM; Hitachi S4800) equipped with energy-dispersive x-ray spectroscopy (EDS), respectively. XRD analysis was operated at 40 kV and 40 mA. Step scans were taken in the range of 2θ = 20°–80° with a 0.02-step, 0.1°/s scan speed and a 2-s exposure. The Rietveld method was adopted to quantitative analysis using DIFFRAC TOPAS 5.0.

RESULTS AND DISCUSSION

Figure 2 shows the XRD patterns of the samples before and after oxidation for 10 h. It showed that the PIRAC-prepared Cr_3Si-Cr_7C_3 outer layer was mainly composed of Cr_3Si and Cr_7C_3 along with a small amount of Cr_3C_2. After oxidation at 1300°C for 10 h, Cr_2O_3 and SiO_2 were detected for the both oxidations. Quantitative analysis on XRD data showed the weight ratios of Cr_2O_3 to SiO_2 in the wet air oxidation condition and the dry air oxidation condition were 13.7 and 29.6, respectively. Distinct lower weight ratios of Cr_2O_3 to SiO_2 in the wet air oxidation condition indicated that there was a larger amount of SiO_2 formed, suggesting that the wet air oxidation condition enhanced the formation of SiO_2.

Figure 3 shows the surface morphologies of the Cr_3Si-Cr_7C_3/SiC/SiC-coated samples before and after oxidation for 10 h. It can be seen that the surface morphologies of the oxidized samples were different from each other and from that of the as-received coating. The as-received Cr_3Si-Cr_7C_3 outer layer exhibited a uniform folded ridge morphology, as shown in Fig. 3a. After the dry air oxidation, the surface showed a relatively loose morphology with many pores. After the wet air oxidation, the surface showed an undulating and loose morphology with notable damage at the position of the bulges, as shown in Fig. 3c.

Figure 4 shows the weight changes during oxidation in the two environments. It can be seen from the figure that the samples showed nonlinear weight gains for both oxidation conditions, with a
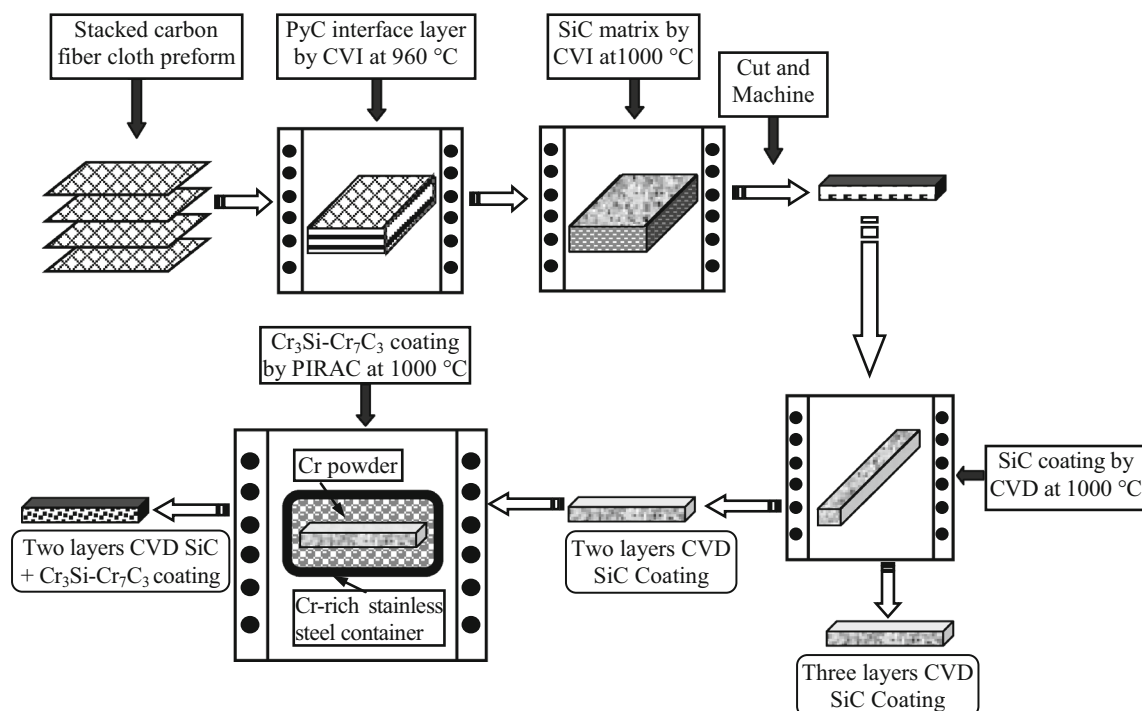
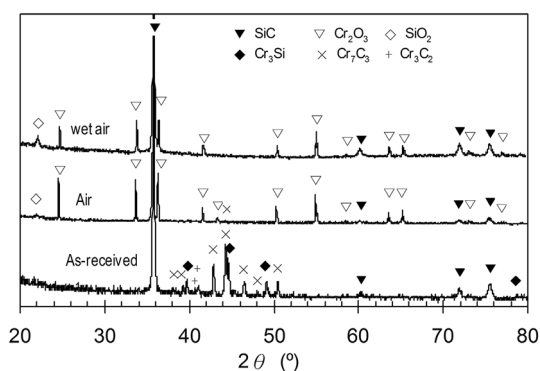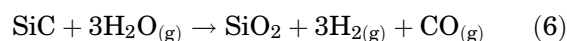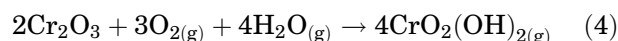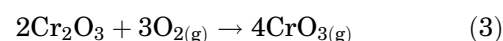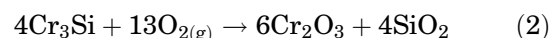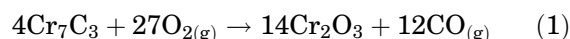Fig. 1. Schematic of samples fabrication processes.

Fig. 2. XRD patterns of the samples before and after oxidation at 1300°C for 10 h.

very rapid weight gains within the first 1 h followed by gradual weight gains thereafter. However, it should be noted that, during the wet air oxidation, the initial rapid weight gains are slightly higher, while the following gradual weight gains are much less. When the oxidation is over 1.75 h, the weight gains induced by the dry air oxidation are larger than those induced by the wet oxidation. The above results are different to those of iron-chromium-aluminum alloys (FeCrAl), of which the oxidation weight gains in dry air condition were faster than in wet air condition.[14]

Figure 5 shows the cross-section morphologies of the $Cr_3Si-Cr_7C_3$/SiC/SiC-coated samples before and after oxidation for 10 h. It was observed that the PIRAC-prepared $Cr_3Si-Cr_7C_3$ outer layer was homogeneous and well-bonded to the CVD SiC/SiC coatings. After dry air oxidation for 10 h, the outer layer

showed a double-layered structure, although the outer layer was homogeneous and well-bonded to the CVD SiC/SiC coatings. After wet air oxidation for 10 h, the outer layer was rough and loose, indicating apparently vaporization. However, it should be noted that there is scarcely discernible oxidation under the coating, as shown in Fig. 5d, indicating that oxidation is taking place on the surface during the two oxidations.

In the present work, possible reactions for the coatings are as follows: [11,15,19–26]

$$4Cr_7C_3 + 27O_{2(g)} \rightarrow 14Cr_2O_3 + 12CO_{(g)} \quad (1)$$

$$4Cr_3Si + 13O_{2(g)} \rightarrow 6Cr_2O_3 + 4SiO_2 \quad (2)$$

$$2Cr_2O_3 + 3O_{2(g)} \rightarrow 4CrO_{3(g)} \quad (3)$$

$$2Cr_2O_3 + 3O_{2(g)} + 4H_2O_{(g)} \rightarrow 4CrO_2(OH)_{2(g)} \quad (4)$$

$$2SiC + 3O_{2(g)} \rightarrow 2SiO_2 + 2CO_{(g)} \quad (5)$$

$$SiC + 3H_2O_{(g)} \rightarrow SiO_2 + 3H_{2(g)} + CO_{(g)} \quad (6)$$

At high temperatures, oxidation of Cr_7C_3 led to the formation of Cr_2O_3 and CO according to reaction (1).[22] Oxidation of Cr_3Si led to the formation of Cr_2O_3 and SiO_2, according to reaction (2).[23, 24] On the other hand, in the present work, the formed Cr_2O_3 may volatilize due to further reacting with oxygen to form gaseous CrO_3, according to reaction (3)[25,26] or water vapor to form gaseous $Cr(OH)_x$,
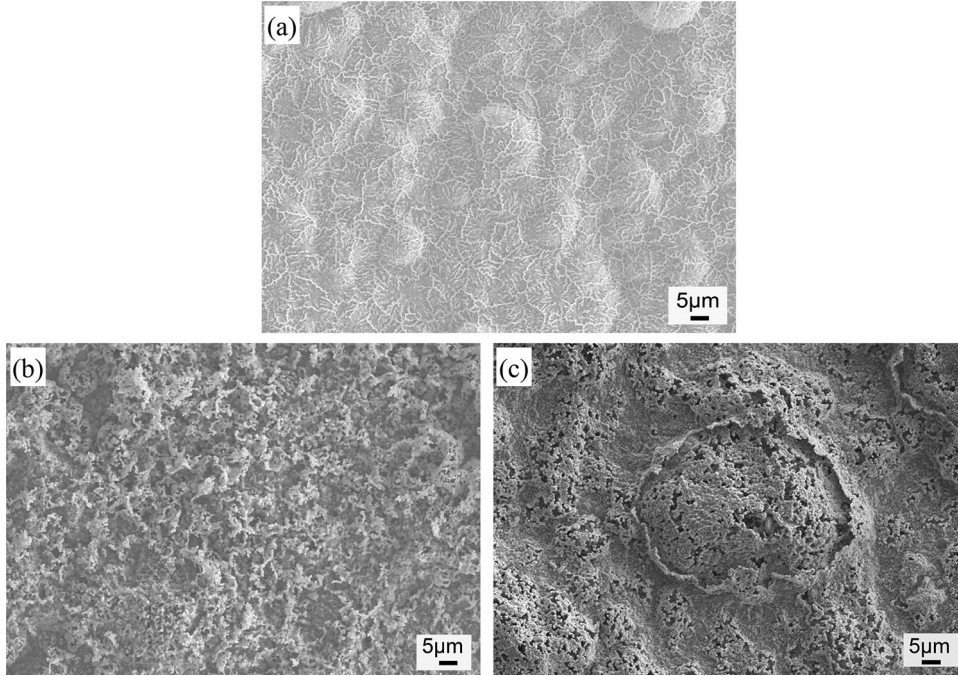
Fig. 3. Surface morphologies of the Cr_3Si-Cr_7C_3/SiC/SiC coated samples before and after oxidation for 10 h: (a) as-received, (b) dry air, and (c) wet air.
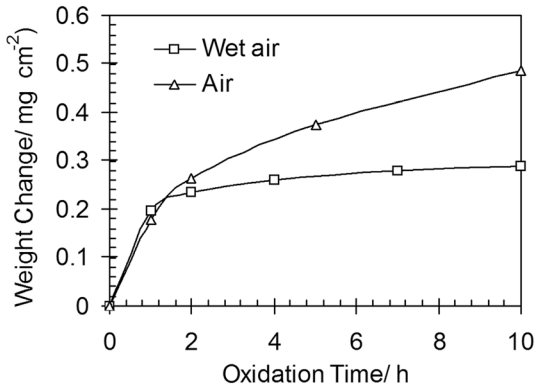

Fig. 4. The oxidation-induced weight changes in the two environments.

according to the reaction (4)[19, 20] Oxidation of SiC led to the formation of SiO_2 and CO, according to reactions (5) and (6).[15]

If there is no oxide volatilization, the oxidation-induced weight gains should be parabolic oxidation, as in Eq. 7:[27]

$$x = k_p \cdot t^{\frac{1}{2}} \qquad (7)$$

where x is the weight gain per unit surface area induced by oxide formation, k_p is the parabolic oxidation rate constant and t is the time.

Figure 6 shows the log–log plot of oxidation-induced weight gains and time for both oxidation conditions. From the results, during the dry air oxidation, the weight gains, Δw_{gain}, and time, t, can be described by:

$$\log(\Delta w_{gain}) = 0.4284 \log(t) - 0.7305 \qquad (8a)$$

$$\text{i.e., } \Delta w_{gain} = 0.18599 \cdot t^{0.4284} \qquad (8b)$$

As the exponent of 0.4284 is lower than 0.5 for parabolic kinetics, it is suggested that there is oxide volatilization during the air oxidation. In the same way, there is oxide volatilization during the wet air oxidation. In these cases, the weight gains versus time should follow a paralinear model, as in Eq. 9 [26]:

$$t = \frac{k_p}{2k_l^2}\left[-\frac{2k_l}{k_p}x - \ln\left(1 - \frac{2k_l}{k_p}x\right)\right] \qquad (9)$$

where k_l is the linear rate constant for oxide volatilization, x is the weight gain per unit surface area induced by oxide formation, k_p is the parabolic oxidation rate constant and t is the time.

Figure 7 shows the comparison of the fitted weight gains, which were calculated according to Eq. 9, and the measured weight gains. It seems that the weight gains can be well-fitted by the paralinear model for both oxidation conditions. In the air oxidation condition, the calculated parabolic rate constant for oxide formation and the linear rate constant for oxide volatilization were 0.03918 $mg^2(cm^{-4} \ h^{-1})$ and 0.02016 $mg(cm^{-2} \ h^{-1})$, respectively. It has been reported that the calculated parabolic rate constant and the linear rate constant of Ni-30Cr at 1300°C in dry air oxidation condition were 0.0882 $mg^2(cm^{-4} \ h^{-1})$ and 0.045 $mg(cm^{-2} \ h^{-1})$, respectively.[25] As the SiO_2 layer reduced the inward diffusion of O and the outward
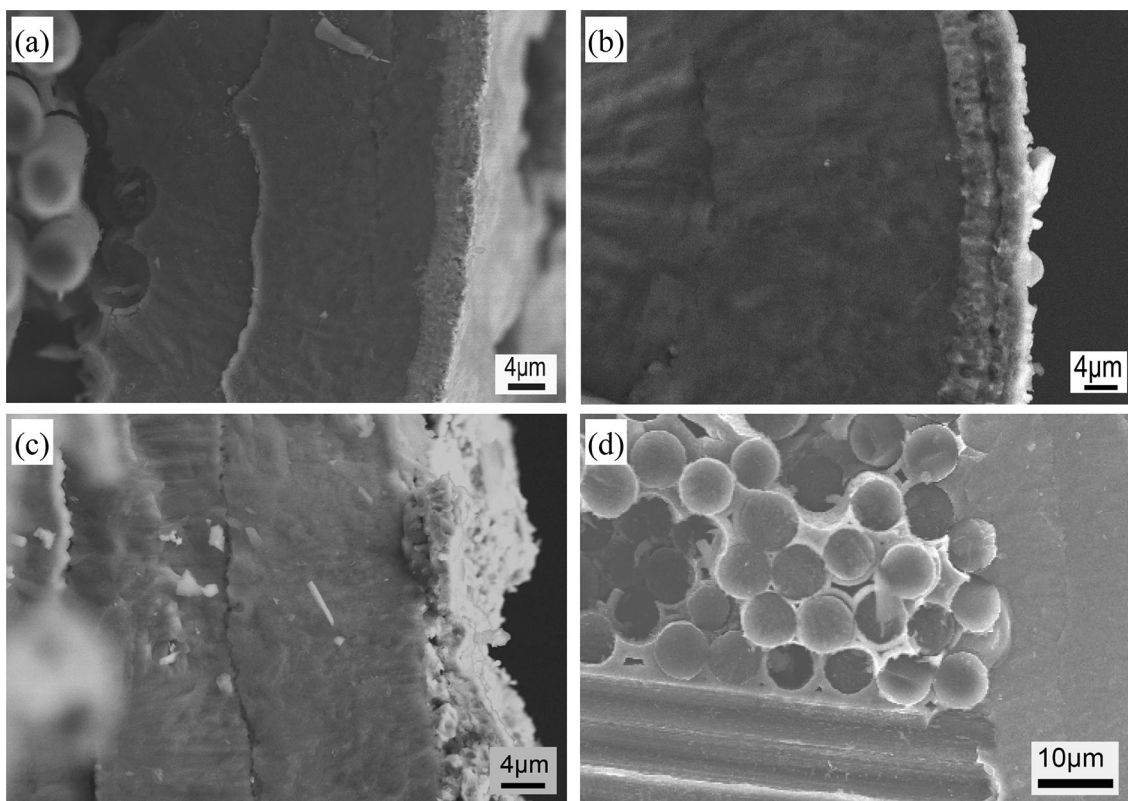
Fig. 5. Cross-section morphologies of the Cr_3Si-Cr_7C_3/SiC/SiC coated samples before and after oxidation for 10 h: (a) as-received, (b) dry air, (c) wet air, (d) view of sub-coating region of (c).
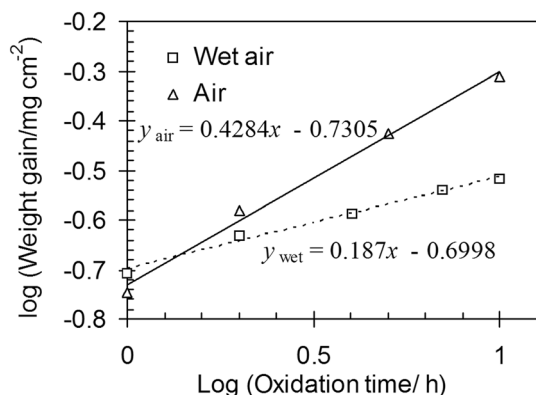

Fig. 6. The log–log plot of weight gains and time during oxidation.

diffusion of Cr,[28] oxide scale growth of the Cr_3Si-Cr_7C_3/SiC/SiC should be lower than that of Ni-30Cr. Moreover, at 1300°C in dry air oxidation condition, SiO_2 is more stable than Cr_2O_3.[15] Therefore, oxidation at 1300°C in dry air, the calculated parabolic rate constant and the linear rate constant of the Cr_3Si-Cr_7C_3/SiC/SiC are all lower than those of the Ni-30Cr.

In the wet air oxidation condition, the calculated parabolic rate constant for oxide formation and the linear rate constant for oxide volatilization were 0.07194 $mg^2(cm^{-4}\ h^{-1})$ and 0.1248 mg $(cm^{-2}\ h^{-1})$, respectively. High parabolic rate constant for oxide formation in the wet air oxidation condition indicates that oxidation of the coating in the wet air
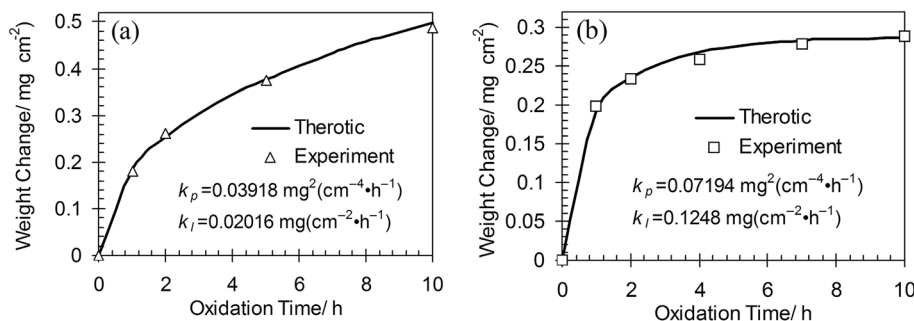

Fig. 7. Comparison of the fitted weight gains and the measured weight gains.

oxidation condition is higher than that in the dry air oxidation condition, and thus there is a higher weight gain rate at the initial oxidation. The calculated linear rate constant for oxide volatilization for the wet air oxidation condition was much higher than that in the air oxidation condition, indicating that water vapor enhances the oxide volatilization and makes the weight gain more gradual. Based on these calculation results and the surface morphology shown in Fig. 3c, and the pores and dilapidation observed on the oxidized surface, it can be concluded that oxide volatilization occurred. The combination the surface morphology and the fine gap observed on the cross-section, it can be concluded that there are gases formed at the oxide/Cr_3Si-Cr_7C_3 interface.[18,21]

It has been well-confirmed that water vapor can enhance oxidizing agent diffusion in chromia and silica, and thus enhance the oxidation rate and formation of chromia and silica.[13,17,18,29–31] Therefore, the rate of weight gain at the initial stage in the wet air oxidation condition was higher than that in the dry air oxidation condition, which was similar to the parabolic rate constant for oxide formation. On the other hand, water vapor can significantly enhance the evaporation of chromia by the formation of gaseous $Cr(OH)_x$.[19,20] Moreover, gaseous $Cr(OH)_x$ will simultaneously be formed in the oxide films due to the transport of OH^- ions (ionic radius of OH^-: 95×10^{-12} m) through the Cr_2O_3 scale being much faster than that of the O^{2-} ionic (ionic radius of O^{2-}: 140×10^{-12} m).[29,32] For the same conditions, gaseous $Cr(OH)_x$ has a higher vapor pressure than $CrO_3(g)$.[33] Consequently, the linear rate constant for oxide volatilization in the wet air oxidation condition was much higher than that in the air oxidation condition, while the oxidation kinetics in the wet oxidation condition showed apparently higher gradual weight gains after the initial rapid weight gains. Meanwhile, the oxidation kinetics in the dry air and the wet air oxidation conditions at 1300°C of Cr_3Si-Cr_7C_3/SiC/SiC are opposite to those of iron-chromium-aluminum alloys (FeCrAl). It has been demonstrated that, at low gas velocity and low pressure, silica volatilization and the corresponding steady-state recession rate are negligible.[34] Therefore, the weight ratio of Cr_2O_3 to SiO_2 in the ratio of the intensity of the SiO_2 peaks to that of the SiC peaks for the wet air oxidation condition was smaller than that for in the dry air oxidation condition.

During oxidation at 1300°C, Cr_2O_3 and SiO_2 coexisted in the oxide film, which was solid-state. Therefore, evaporation of the external portion of the Cr_2O_3 scale resulted in the air-oxidized surface showed a relatively rough loose morphology with many pores, as shown in Fig. 3b. During the wet oxidation, the water vapor resulted in viscous silica being formed,[13,35,36] which resulted in the release of the $Cr(OH)_x$ formed in the oxide films and at the oxide/Cr_3Si-Cr_7C_3 interface being baffled. As a result, the escape of gases induced local bulging and damage to the oxides film, as shown in Fig. 3c.

CONCLUSIONS

Oxidation kinetics of a Cr_3Si-Cr_7C_3/SiC/SiC-coated C/SiC composite was comparatively investigated in dry air and wet air.

After oxidation at 1300°C for 10 h, the produced phases were Cr_2O_3 and SiO_2 for the two oxidation conditions. However, a larger amount of SiO_2 formed in the wet air oxidation condition. Both oxidations made the surface of Cr_3Si-Cr_7C_3/SiC/SiC coating become relatively loose with many pores. After the wet air oxidation, enhanced evaporation of gases caused the surface of the Cr_3Si-Cr_7C_3/SiC/SiC coating to showed notable damage at the position of bulges.

The Cr_3Si-Cr_7C_3/SiC/SiC-coated C/SiC composite showed paralinear weight gains during both oxidation environments. Although the rapid weight gains within the first 1 h in the wet air oxidation condition were higher, the gradual weight gains thereafter were lower.

In the dry air oxidation condition, the calculated parabolic rate constant for oxide formation and the linear rate constant for oxide volatilization were 0.03918 mg^2 (cm^{-4} h^{-1}) and 0.02016 mg (cm^{-4} h^{-1}), respectively. In the wet air oxidation condition, the calculated parabolic rate constant for oxide formation and the linear rate constant for oxide volatilization were 0.07194 mg^2(cm^{-4} h^{-1}) and 0.1248 mg (cm^{-4} h^{-1}), respectively.

REFERENCES

1. R. Naslain and F. Christin, *MRS Bull.* 28, 654 (2003).
2. S. Schmidt, S. Beyer, H. Knabe, H. Immich, R. Meistring, and A. Gessler, *Acta Astronaut.* 55, 409 (2004).
3. J. Swain, K. Gaurav, D. Singh, P.K. Sen, and S.K. Bohidar, *Inter. J. Innov. Res. Sci. Technol.* 1, 290 (2014).
4. A. Sommers, Q. Wang, X. Han, C. T'Joen, Y. Park, and A. Jacobi, *Appl. Therm. Eng.* 30, 1277 (2010).
5. W. Krenkel, *Inter. J. App. Ceram. Technol.* 1, 188 (2004).
6. J.R. Strife and J.E. Sheehan, *Ceram. Bull.* 67, 369 (1998).
7. F.J. Buchanan and J.A. Little, *Corros. Sci.* 35, 1243 (1993).
8. W. Li, Y. Xiang, B.F. Zhang, S. Wang, J. Liu, Q.G. Lin, and J. Yang, *Corros. Sci.* 74, 149 (2013).
9. S.J. Wu, L.F. Cheng, L.T. Zhang, and Y.D. Xu, *Surf. Coat. Technol.* 200, 4489 (2006).
10. L. Li, H.J. Li, H.J. Lin, L. Zhuang, S.L. Wang, T. Feng, X.Y. Yao, and Q.G. Fu, *Surf. Coat. Technol.* 302, 56 (2016).
11. S.J. Wu, Y.G. Wang, Q. Guo, B. Guo, and L. Luo, *Mater. Sci. Eng., A* 644, 268 (2015).
12. E.J. Opila, *J. Am. Ceram. Soc.* 82, 625 (1999).
13. S.J. Wu, L.F. Cheng, and L.T. Zhang, *Corros. Sci.* 66, 111 (2013).

14. R.B. Rebak, V.K. Gupta, and M. Larsen, *JOM* 70, 1484 (2018).
15. E.J. Opila, N.S. Jacobson, D.L. Myers, and E.H. Copland, *JOM* 58, 22 (2006).
16. S.J. Wu, B. Guo, T.B. Li, and D.M. Gui, *Constr. Build. Mater.* 81, 11 (2015).
17. N.K. Othman, J.Q. Zhang, and D.J. Young, *Corros. Sci.* 52, 2827 (2010).
18. Y.P. Jacob, V.A.C. Haanappel, M.F. Stroosnijder, H. Buscail, P. Fielitz, and G. Borchardt, *Corros. Sci.* 44, 2027 (2002).
19. A. Yamauchi, K. Kurokawa, and H. Takahashi, *Oxid. Met.* 59, 517 (2003).
20. H. Asteman, J.E. Svensson, and L.G. Johansson, *Corros. Sci.* 44, 2635 (2002).
21. N.K. Othman, N. Othman, J. Zhang, and D.J. Young, *Corros. Sci.* 51, 3039 (2009).
22. Y.N. Kok and P.E.H. Hovsepian, *Surf. Coat. Technol.* 201, 3596 (2006).
23. J.H. Ma, Y.L. Gu, L. Shi, L.Y. Chen, Z.H. Yang, and Y.T. Qian, *J. Alloy. Compd.* 375, 249 (2004).
24. S.V. Raj, *Mater. Sci. Eng., A* 192–193, 583 (1995).
25. P. Berthod, *Oxid. Met.* 64, 235 (2005).
26. C.S. Tedmon, *J. Electrochem. Soc.* 113, 766 (1967).
27. C. Wagner, *J. Electrochem. Soc.* 99, 369 (1952).
28. P. Tunthawiroon, Y.P. Li, N. Tang, Y. Koizumi, and A. Chiba, *Corros. Sci.* 95, 88 (2015).
29. J. Ehlers, D.J. Young, E.J. Smaardijk, A.K. Tyagi, H.J. Penkalla, L. Singheiser, and W.J. Quadakkers, *Corros. Sci.* 48, 3428 (2006).
30. J. Zurek, D.J. Young, E. Essuman, M. Hänsel, H.J. Penkalla, L. Niewolak, and W.J. Quadakkers, *Mater. Sci. Eng., A* 477, 259 (2008).
31. B.E. Deal and A.S. Grove, *J. Appl. Phys.* 36, 3770 (1965).
32. H. Nickel, Y. Wouters, M. Thiele, and W.J. Quadakkers, *J. Anal. Chem.* 361, 540 (1998).
33. G.R. Holcomb, *Oxid. Met.* 69, 163 (2008).
34. E.J. Opila, *J. Am. Ceram. Soc.* 86, 1238 (2003).
35. B.B. Karki and L. Stixrude, *Phys. Rev. Lett.* 104, 215901 (2015).
36. S.J. Wu, L.F. Cheng, J. Zhang, L.T. Zhang, X.G. Luan, H. Mei, and P. Fang, *Mater. Sci. Eng., A* 435–436, 412 (2006).